Microelectronic Engineering 228 (2020) 111332

Contents lists available at ScienceDirect

Microelectronic Engineering

journal homepage: www.elsevier.com/locate/mee

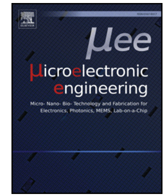

Research paper

Technology and optimization of hafnium oxynitride (HfO_xN_y) thin-films formed by pulsed-DC reactive magnetron sputtering for MIS devices

Mirosław Puźniak[a,b,*], Wojtek Gajewski[b], Marcin Żelechowski[b], Jan Jamroz[c], Arkadiusz Gertych[c], Mariusz Zdrojek[c], Robert Mroczyński[a]

[a] Warsaw University of Technology, Institute of Microelectronics and Optoelectronics, Koszykowa 75, 00-662 Warsaw, Poland
[b] TRUMPF Huettinger, Marecka 47, 05-220 Zielonka, Poland
[c] Warsaw University of Technology, Faculty of Physics, Koszykowa 75, 00-662 Warsaw, Poland

ARTICLE INFO

Keywords:
High-k dielectric
Reactive magnetron sputtering
Thermal stability
Electrical parameters
Structural characterization

ABSTRACT

This study is devoted to the technology and optimization of pulsed-DC reactive magnetron sputtering of hafnium oxynitride (HfO_xN_y) thin-films. The fabrication process of HfO_xN_y films was optimized employing the Taguchi orthogonal tables approach leading to the material with possible best electrical parameters. During the optimization procedure, the parameters of dielectric films were monitored by means of electrical characterization of MIS structures with hafnium oxynitride as the gate-dielectric. The thermal stability of fabricated HfO_xN_y layers was also examined. The presented results have shown the improved electrical parameters of fabricated films after thermal treatment. Namely, we have observed beneficial flat-band voltage (V_{fb}) value, the disappearance of frequency dispersion of C−V characteristics, reduced effective charge (Q_{eff}/q), and interface traps (D_{it}) densities of examined MIS structures. However, the permittivity value is slightly lower as compared to reference samples. The superior stability of HfO_xN_y layers up to 800 °C was proved. Although the significant increase of crystalline phase in the layer bulk was observed, no deterioration of electrical properties or surface morphology has been noticed. The results presented in this study make the investigated HfO_xN_y fabricated using pulsed-DC reactive magnetron sputtering the possible candidate as a gate dielectric in MIS structures and devices.

1. Introduction

Even though hafnia-based dielectric materials have already replaced thermal silicon dioxide (SiO_2) or oxynitride (SiO_xN_y) as the gate dielectric in nowadays Ultra-Large Scale Integration (ULSI) devices, there are still many important aspects to be understood and study for hafnium oxide materials technology and processing [1]. Thermal stability is one of the many critical issues as several high-temperature steps are performed after depositing the gate dielectric which strongly influences the electrical properties of the deposited dielectric films [2]. Several high-*k* materials are investigated for applications in modern electronics and photonics, but hafnium oxide (HfO_2) is the most examined material due to its relatively large permittivity value [3], large band-gap [4], reasonably good band offset in contact with silicon substrate [5], and demonstrated compatibility with poly-silicon, as well as metal gate electrodes [6,7]. What is commonly known, the HfO_2 exhibits strongly suppressed gate tunneling current as compared to silicon dioxide or oxynitride [8] that makes such film feasible as gate-dielectric material in Metal-Insulator-Semiconductor (MIS) structures. However, the crystallization temperature of hafnium dioxide is relatively low and it leads to the increase of the formation of grain boundaries which are excellent paths for oxygen, boron, and other impurities penetration into the semiconductor/dielectric interface. These effects have to be reduced in order to maintain reasonably low Equivalent Oxide Thickness (EOT), leakage current density, and flat-band voltage (V_{fb}) fluctuations that may degrade the particular device quality and performance [9,10].

Recently, several works have considered the hafnium oxynitride (HfO_xN_y) as a promising dielectric material for the applications in modern semiconductor devices, as the incorporation of nitrogen into the dielectric layer bulk results in the increase of the crystallization temperature [11]. Numerous methods for the fabrication of hafnium oxynitride films can be used, i.e. high-temperature reoxidation of physically vapor deposited (PVD) hafnium nitride (HfN) to form HfO_xN_y, Chemical Vapor Deposition (CVD), or metalorganic chemical vapor deposition (MOCVD) [12–14]. However, the reactive magnetron sputtering process seems to be a very attractive method of the fabrication as the synthesis offers many advantages, such as low-temperature processing (i.e. at room temperature), good uniformity, and purity

* Corresponding author at: Warsaw University of Technology, Institute of Microelectronics and Optoelectronics, Koszykowa 75, 00-662 Warsaw, Poland.
E-mail address: miroslaw.puzniak@trumpf.com (M. Puźniak).

https://doi.org/10.1016/j.mee.2020.111332
Received 23 April 2020; Accepted 29 April 2020
Available online 06 May 2020
0167-9317/ © 2020 Elsevier B.V. All rights reserved.

of the deposited material, as well as good control over stoichiometry and quality upon the sputtering's parameters [15,16].

In this work, the optimization of the technology of HfO_xN_y deposited using pulsed-DC reactive magnetron sputtering process was presented. The experimental runs were designed according to the Design of Experiments (DoE) method, namely Taguchi orthogonal tables [17]. DoE is a methodology for systematically applying statistics to experimentation [18]. It can also be defined as a series of tests in which purposeful changes are made to the input variables of a process or system so that one may observe and identify the reasons for these changes in the output response [19]. Numerous case studies in different areas of application prove the advantages and potential of DoE methods, such as Block Designs, Two-Level/General/Fractional Factorial Experiments, Response Surface Methodology, or Evolutionary Algorithms [20–22]. However, the use of orthogonal tables by means of the Taguchi approach is easy to implement, quite effective, allows for a large saving in an experimental effort, and simple in the analysis. Therefore, orthogonal tables have already found number of implementations in environmental [23], and agricultural sciences [24], physics [25], chemistry [26], statistics [27], management and business [28], or medicine [29].

The DoE method used in this study allowed for the effective reduction of a number of experiments to be performed to check the dependencies between variables of process' parameters, i.e. magnetron sputtering in this case and output parameters, i.e. the properties of the investigated material or structure [30]. As a consequence of the optimization process, the set of variables of reactive magnetron sputtering process was designed giving the HfO_xN_y film with the best possible electrical parameters. The changes in the properties of obtained films during the optimization procedure were monitored employing spectroscopic ellipsometry and electrical characterization of purposely fabricated MIS structures. The thermal stability of hafnium oxynitride layers was also examined. The structural parameters and surface morphology of dielectric films were investigated by means of Atomic Force Microscopy (AFM) and Grazing-Angle Incidence X-Ray Diffraction (GIXRD) technique. Finally, we presented the superior thermal stability of the hafnium oxynitride layer up to 800 °C that makes the fabricated films the possible candidates as the gate dielectric material in MIS structures and devices.

2. Experimental

The HfO_xN_y films have been fabricated on (100) p-type silicon (Si) substrates with the resistivity of 1 ÷ 10 Ωcm using pulsed-DC reactive magnetron sputtering process using PlasmaLab System 400 made by Oxford Instruments Plasma Technology. Prior to the fabrication of dielectric films, Si substrates have been cleaned by means of modified Radio Corporation of America (RCA) method (piranha + SC1 + SC2 + BHF dipping). The experimental part was divided into three stages.

The first stage aimed to investigate the influence of sputtering process' parameters onto the kinetics growth and electrical properties of HfO_xN_y films. For this reason, MIS capacitors with hafnium oxynitride films, as the gate dielectric material, have been fabricated. As it was mentioned above, the experimental runs were prepared according to the Taguchi orthogonal tables. In this work, the $L_9(3)^4$ table was used. This orthogonal table assumes the investigation of the influence of four process parameters, each with three variables, onto the output properties. The number of processing steps was 9. The influence of power applied to the electrodes, pressure in the reactive chamber, argon, and nitrogen flow onto the thickness and electrical properties of fabricated films were considered in this study. The time of the process in each processing step was kept constant at 5 min. Table 1 presents the selected values of process' parameters for the optimization of electrical properties of hafnium oxynitride thin films, that are investigated in this study.

Table 1
Selected values of pulsed-DC reactive magnetron sputtering process' selected for the optimization of electrical properties of HfO_xN_y films.

Pressure (mTorr)	DC power (W)	Oxygen flow (sccm)	Argon flow (sccm)
3	100	5	5
6	300	10	10
9	500	15	15

The obtained results allowed for the selection of the most promising parameters in order to obtain the dielectric layer with tailored properties. Thus, in the second stage of the experimental part, the verification of the optimization procedure has been carried out and the two sets of sputtering parameters have been designed in order to obtain a dielectric material, i.e. (1) with the possible best, and (2) the worst electrical parameters. The aim of this procedure was to show that the optimization using the Taguchi approach has been performed successfully and the fabrication of dielectric films is controllable. In this step we have adjusted the time of the process to obtain a dielectric film with the thickness ~ 30 nm.

In the third stage, the MIS structures have been fabricated using the optimized process of HfO_xN_y fabrication. Split experiments with annealing of obtained structures have been performed by the use of the standard furnace at 300 °C and 800 °C in the argon atmosphere for 30 min. After the annealing, the magnetron sputtering process was also used to fabricate aluminum (Al) which was used as the top-metal gate. The standard photolithography process using the wavelength 400 nm was used to pattern the Al contacts. And thus the MIS structures were divided into the 'reference' – without any annealing treatment, and annealed at 300 °C and 800 °C.

The electrical measurements of fabricated structures were performed with the Keysight B1500 and Keithley 4200 semiconductor characterization system equipped with SUSS PM-8 probe station. The MIS capacitors with the gate area of $A = 1.8 \times 10^{-4}\,cm^2$ were used, allowing the determination of the basic electrical properties of the investigated stacks. Possible changes in the electrical parameters were investigated through capacitance-voltage (C—V), as well as current-voltage (I-V) measurements. The methodology of the estimation of electrical parameters of the fabricated MIS test structures was described previously in [31]. The electrical measurements were done using around 15 test capacitors of each type of examined MIS device. All presented characteristics in the manuscript are representative ones. The changes in structure and chemical composition of investigated semiconductor/dielectric system were studied by means of spectroscopic ellipsometry, Atomic Force Microscopy, and Grazing-Angle Incidence X-Ray Diffraction technique. The thickness and optical properties of investigated hafnium oxynitride thin-films were determined using Jobin-Yvon UVISEL spectroscopic ellipsometer in a wavelength range from 190 nm to 850 nm. Grazing Incidence X-Ray Diffraction data were collected on a PANalytical Empyrean Series 2 diffractometer, fitted with an PIXcel^{3D} detector, using Cu-Kα radiation ($\lambda_1 = 1.54056$ Å and $\lambda_2 = 1.54439$ Å). Data collections were performed in the 2θ range 10–80°, in steps of 0.0131°, with an effective scan time of 200 s per step. Incidence angle was set as $\omega = 0.4°$. Those parameters were selected as the maximum intensity of the signal from the HfO_xN_y, and the minimum signal from the semiconductor substrate was observed. Phases were identified with HighScore Plus suite. The surface morphology characterization was done using Bruker Dimension Icon microscope in tapping mode. The images of the dimensions 5 μm × 5 μm were collected in order to evaluate the topography of examined materials and calculate their roughness as root-mean-square (RMS) values.

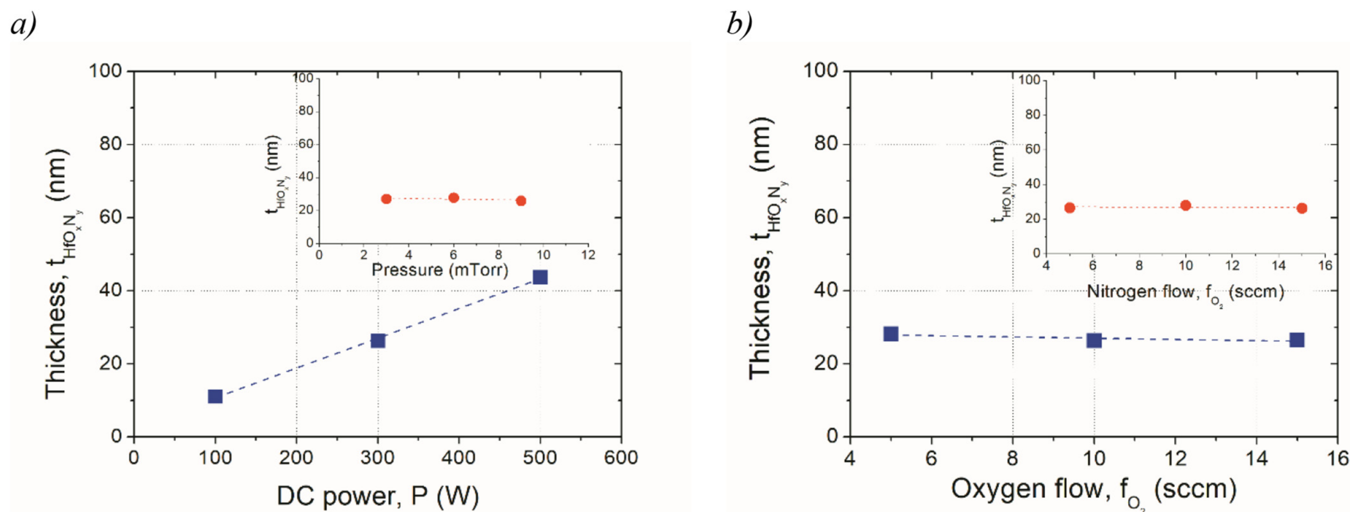

Fig. 1. Influence of reactive magnetron sputtering process' parameters onto kinetics growth of HfO_xN_y films; influence of the pressure in reactive chamber and nitrogen flow have been depicted as the insets.

3. Results and discussion

3.1. Investigations of the influence of sputtering process' parameters onto the growth and electrical properties of HfO_xN_y films

Before the fabrication of MIS structures, in the first stage of optimization, the influence of the input process' parameters (i.e. pressure in the reactive chamber, DC power, and O_2/N_2 flow) onto output parameters (i.e. thickness and electrical properties of obtained dielectric films) was analyzed. It allowed for the selection of the most promising values of sputtering parameters to fabricate the high-*k* films with the best electrical properties. The first set of experimental runs within the 1st stage of optimization procedure allowed for the fabrication of dielectric material in the range of 10 ÷ 46 nm. The time of the process in each processing step was kept constant at 5 min. The influence of the sputtering's parameters onto the kinetic growth of dielectric materials has been depicted in Fig. 1.

The results presented in Fig. 1 were shown according to the analysis of data in the DoE method. Based on this method, these results can be considered as not exact dependences, but the trends between selected input and output parameters. It is reasonable to conclude that in the range of selected variables of sputtering's parameters, the power applied to the electrodes is the most influential onto the ultimate thickness of HfO_xN_y films, as the increase of DC-power results in the noticeable increase of thickness (see Fig. 1a). The remaining parameters can be neglected during the further optimization, as the change of pressure, and reactive gases flow onto the thickness is not significant (Fig. 1b) in this range.

In order to check the influence of the magnetron sputtering's parameters onto the electrical parameters of investigated dielectric layers, the MIS structures with HfO_xN_y film act as gate-dielectric were fabricated. In this step, the time of each processing step was adjusted to obtain a dielectric film with a similar thickness of the order of 30 nm. A similar analysis of the trends between process' parameters and basic electrical parameters of obtained MIS structures has been performed. As an example, the trends showing the changes in sputtering's parameters and effective charge density (Q_{eff}/q) or relative permittivity (*k*) values have been illustrated in Fig. 2. The data presented in Fig. 2 have taken into account the electrical parameters of as-deposited and annealed at 300 °C HfO_xN_y films.

By the analysis of the results shown in Fig. 2, it can be assumed that the annealing at 300 °C results in the improvement of electrical parameters of fabricated hafnium oxynitride films. Similar results were obtained in our previous work, which was concentrated on hafnium oxide (HfO_x) layers [32]. In all cases presented in Fig. 2, the annealed material can be characterized by reasonably lower effective charge density and higher relative permittivity, as compared to as-deposited films.

As in the case of the investigation of input parameters' affection onto thickness, DC-power applied to the reactive chamber has the most significant influence on electrical parameters of fabricated films. As demonstrated in Fig. 2a, the increase of the DC-power results in the decrease of the Q_{eff}/q value, and simultaneously, the increase of the relative permittivity of HfO_xN_y film. Such a finding is very beneficial for further optimization, as it shows the specific direction to set a particular variable of DC-power value.

Taking into account the obtained trends between input and output parameters, the comparable trends for as-deposited and annealed layers were also observed. However, only in the case of the influence of pressure onto the relative permittivity, the opposed dependence was observed, i.e. the increase of the pressure results in the noticeably increase, and decrease of the permittivity for as-deposited, and annealed film, respectively. Nevertheless, for the sake of further optimization of hafnium oxynitride films the dependencies obtained for annealed samples have been taken into account as the technology of semiconductor-based structures demands processes that are performed at a higher temperature, thus, the electrical properties of annealed layers are the most important for the ultimate aim of optimization.

The trends illustrated in Fig. 2 can be used for the anticipation of the most promising variables of process' parameters to fabricate HfO_xN_y films with the best possible electrical parameters. As was mentioned previously, the layer should be formed at higher DC-power values, as the effective charge density as well as the permittivity show quite beneficial values (Fig. 2a). In the case of pressure and oxygen flow (Figs. 2b and c), both parameters should be maintained at a possibly low level, while nitrogen flow (Fig. 2d) should be set at a higher value. However, it is worth noting that the particular influence of reactive gases flow shows a lower impact on the basic electrical parameters compared to the power applied onto electrodes and pressure in the reactive chamber.

3.2. Optimization of electrical properties of HfO_xN_y thin-films

Based on the observed trends and the discussion in the 1st stage of optimization, two sets of experimental runs have been designed as follows: (1) with possible the best and (2) worse electrical parameters. In this part of the work, the thickness of HfO_xN_y films was 30 nm in all cases. Such a methodology allowed for the verification of obtained

Fig. 2. Influence of reactive magnetron sputtering process' parameters onto effective charge density and relative permittivity of HfO_xN_y films.

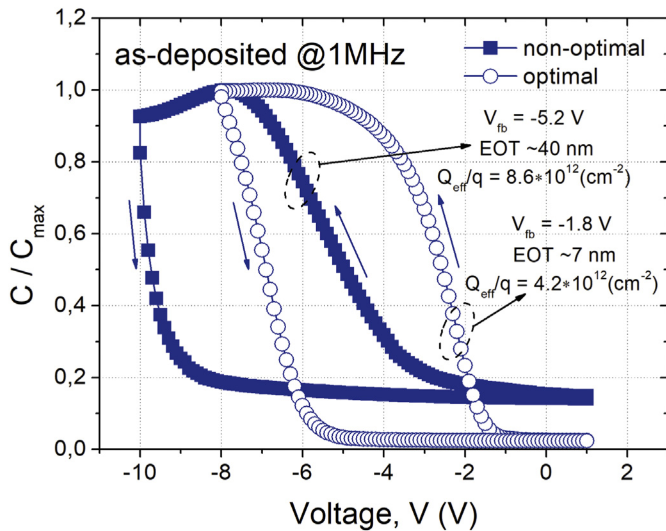

Fig. 3. Comparison of the hysteresis loop of C—V characteristics of MIS structures with HfO_xN_y films fabricated using a designed set of reactive magnetron sputtering's parameters; the purposely designed set of parameters in order to fabricate material with possibly best (optimal), and worst (non-optimal) electrical parameters.

trends in the first stage of optimization. The results of this experiment have been presented in Fig. 3 that depicts the comparison of C—V characteristics of fabricated MIS structures. The results presented in Fig. 3 clearly show that the 'optimal' C—V curve can be characterized by a lower flat-band voltage value (in absolute value), lower Equivalent Oxide Thickness, thus higher permittivity, and lower Q_{eff}/q compared to the structure with HfO_xN_y fabricated by 'non-optimal' process. Both hystereses of C—V characteristics are reasonably large that originate from charge traps located in the HfO_xN_y bulk, i.e. predominantly unsaturated Hf-O-N bonds. However, the hysteresis of the 'non-optimal' structure is significantly higher, and in accumulation regime, a characteristic lowering of the capacitance value is observed that suggests the increase of the leakage current. These results prove the correctness of the methodology used for the optimization and the proper selection of the variables of process' parameters for both types of experimental runs.

Split experiments with the annealing at 300 °C of fabricated MIS structures has been performed. The hysteresis loop and frequency dispersion of obtained C—V characteristics, compared to the curves of the MIS device with the best electrical properties obtained in the 1st stage of optimization, have been depicted in Fig. 4.

The results presented in Fig. 4 suggest that the MIS structures fabricated in the 2nd stage of optimization are characterized by improved electrical properties. Although the hysteresis of both investigated structures is the same (ΔV_{fb} of the order of 1 V), the flat-band voltage value (taken into account in absolute value) and relative permittivity

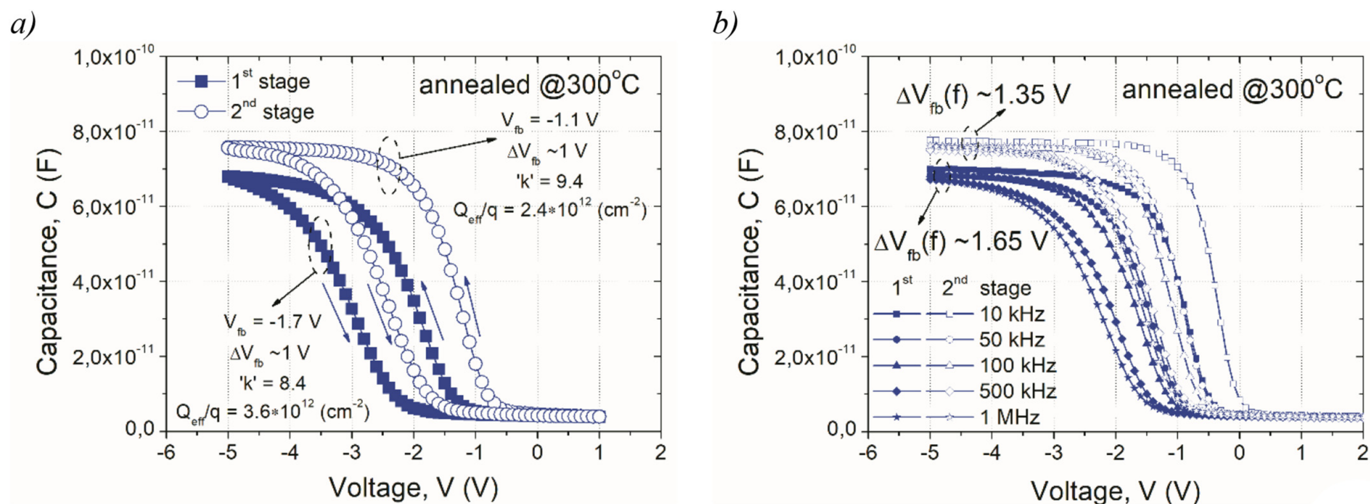

Fig. 4. Comparison of hysteresis loop (a), and frequency dispersion $\Delta V_{fb} = f(f)$ (b) of high-frequency (@1 MHz) C—V characteristics of annealed at 300 °C MIS structures fabricated in the 1st (the best experimental run) and 2nd stage of optimization of electrical properties of hafnium oxynitride layers.

are −1.1 V and 9.8, respectively, that are significantly beneficial compared to the values of MIS structures fabricated in the 1st stage of optimization (Fig. 4a). Moreover, the frequency dispersion of V_{fb}, which has been shown in Fig. 4b is larger for structure fabricated in the 1st stage of optimization suggesting the higher level of charge traps, as was proved by the larger effective charge density, i.e. $8.6 \times 10^{12}\ cm^{-2}$ and $4.2 \times 10^{12}\ cm^{-2}$, estimated from C—V characteristics of structures obtained in the 1st and 2nd stage of optimization, respectively.

Taking into account the results of optimization presented above, it can be concluded that the application of DoE method in the form of Taguchi orthogonal tables allowed for the fabrication of MIS structures with HfO_xN_y layers with improved electrical parameters as compared to the initial stage of examinations. The designed set of parameters of reactive magnetron sputtering process has been used in the investigations of the thermal stability of hafnium oxynitride films.

3.3. Thermal stability and structural properties of hafnium oxynitride layers

In the last part of the experimental, the thermal stability of HfO_xN_y layers has been investigated. The test structures in the form of MIS devices with 30 nm of hafnium oxynitride acts as gate-dielectric were fabricated. Split experiments with annealing of obtained test structures have been performed using the standard furnace at 300 °C and 800 °C in the argon atmosphere for 30 min. The C—V characteristics of fabricated test devices are shown in Fig. 5. The basic electrical parameters evaluated from the C—V characteristics are depicted in Table. 2.

Table 2
Basic electrical parameters estimated from the C—V characteristics analysis of MIS devices.

	Relative permittivity	EOT (nm)	V_{fb} (V)	Q_{eff}/q (cm^{-2})	D_{itmb} ($eV^{-1}\ cm^{-2}$)
As-deposited	10.8	7.5	−1.8	4.3×10^{12}	8.8×10^{12}
Annealed @300 °C	9.4	7.9	−1.1	2.3×10^{12}	2.4×10^{12}
Annealed @800 °C	9.1	8.1	−0.8	1.4×10^{12}	1.3×10^{12}

The significant improvement of electrical parameters of MIS structures as a consequence of the performed annealing of hafnium oxynitride films is demonstrated. Although relative permittivity is a little decreased as compared to as-deposited film (see Table 2), which results in the increase of EOT value from 7.5 nm to 8.1 nm for as-deposited and annealed HfO_xN_y layer, respectively, the other of the electrical parameters are improved. It is worth to emphasize that V_{fb}, Q_{eff}/q, and D_{itmb} values are decreasing as the temperature of annealing increases. The

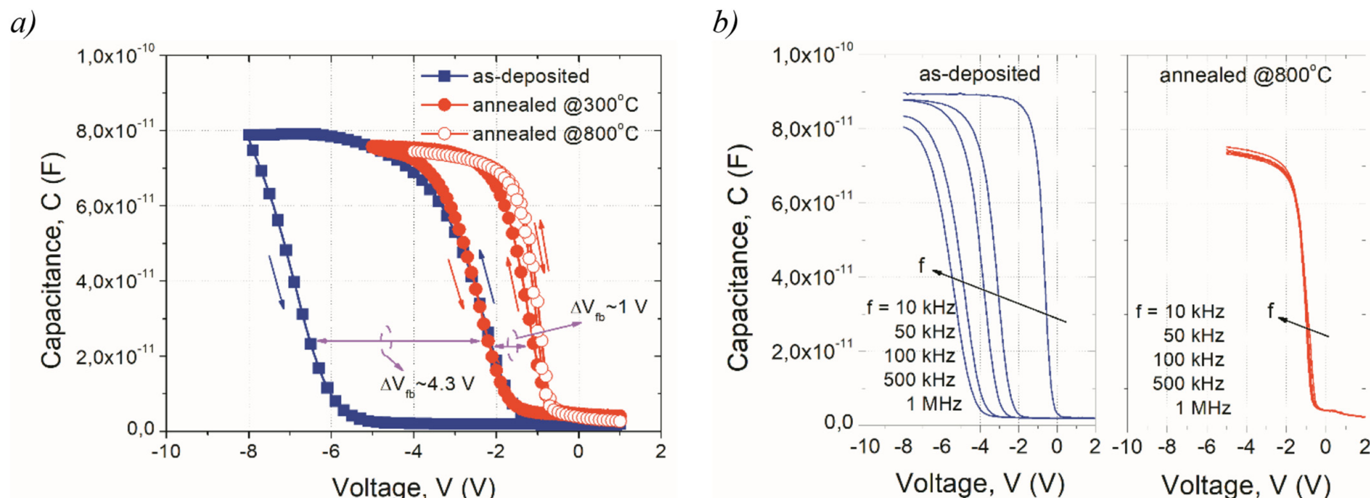

Fig. 5. High-frequency (@1 MHz) C—V characteristics (a) and frequency dispersion of C—V curves (b) of MIS structures with HfO_xN_y before (as-deposited) and after thermal treatment (annealed @300 °C and 800 °C); the direction of the increasing frequency was also shown.

trend with the decrease of '*k*' value was observed in our previous study, in which we dealt with the investigation of the thermal stability of scandium oxide films [33], and it is a result of changes of the nitrogen content and passivation of dangling bonds in the dielectric material bulk due to the thermal treatment [34].

It should also be noted that the comparison of C−V measurements of MIS structures after the annealing shows the superior stability and the complete disappearance of hysteresis (see Fig. 5a), and frequency dispersion of C−V curves (see Fig. 5b), which suggests the best electrical parameters of annealed at 800 °C HfO_xN_y layer. Moreover, for the positive gate bias voltage, the deep depletion phenomenon has been observed. It's believed that in this region, the TAT mechanism dominates the current behavior, thus the carrier tunneling rate through the hafnium oxynitride is sufficiently large. The minority carriers generated in the sub-surface region of semiconductor substrate directly tunnel through the hafnium oxynitride under excess gate bias. When gate bias sweeps through the inversion region too fast, there is no sufficient amount of minority carriers to supply the leakage current to satisfy electrical neutrality. The depletion region becomes broader than that in thermal equilibrium, and the total capacitance decreases below its thermal equilibrium value. A similar phenomenon has been observed in [35] and it usually occurs for the lower intensity of the electric field, as in this case. However, to fully study this phenomenon the comprehensive analysis of the transport mechanisms needs to be done that will be performed in the future.

Furthermore, the measurements of current-voltage characteristics of MIS test structures revealed slightly better insulating properties of annealed HfO_xN_y films compared to the as-deposited dielectric layer. In Fig. 6, the comparison of representative I-V characteristics (shown as the current density vs. electric field intensity) of investigated in this work MIS structures is depicted. It is worth to underline that the measurements were performed towards accumulation regime while the values of electric field intensity are expressed as positive. The I-V curves show relatively lower leakage current density and higher breakdown voltage (V_{br}) value (i.e. ~6.7 MV/cm), as compared to the structure with as-deposited hafnium oxynitride film.

To examine the structural properties of hafnium oxynitride films and try to link both electrical and structural properties, the Grazing Incidence X-Ray Diffraction was performed. The GIXRD patterns of investigated in this work as-deposited and annealed hafnium oxynitride films are depicted in Fig. 7. The examined samples can be divided into two groups due to the structure, i.e. abundant in amorphous and crystalline phases. The as-deposited and annealed at 300 °C sample can

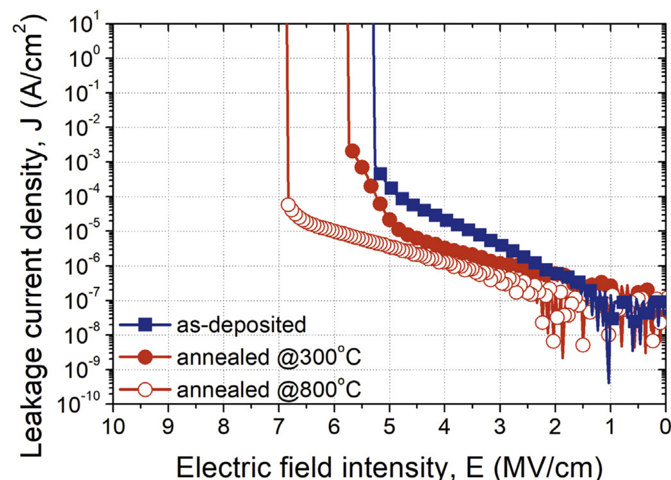

Fig. 6. Comparison of I-V characteristics (expressed as leakage current density vs. electric field intensity) of MIS structures with examined hafnium oxynitride thin-films; the curves were collected towards accumulation regime but the intensity of electric field was depicted as positive.

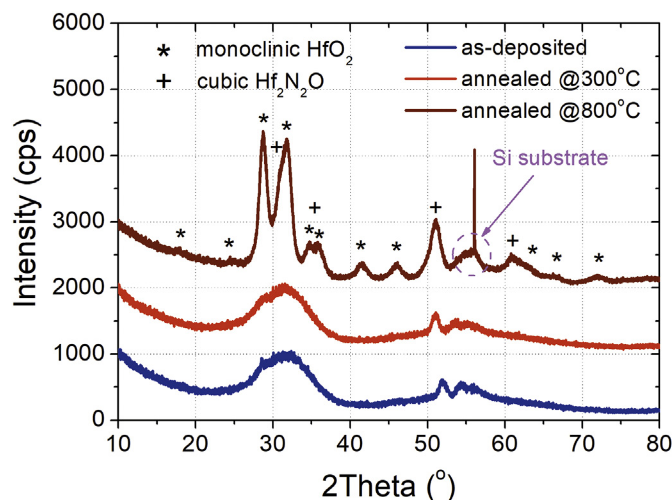

Fig. 7. GIXRD patterns of investigated in this study HfO_xN_y thin-films.

be characterized by a pattern that is typical for amorphous material, although certain reflexes can be observed, e.g. at 2theta ~53°. However, this signal has low intensity and possibly originates from a Si substrate.

On the contrary, the annealed at 800 °C HfO_xN_y can be characterized by a specific crystalline structure. Structural analysis revealed that the dielectric material is most likely composed of two phases, i.e. (1) monoclinic of space group P 1 21/c 1 with the chemical composition of stoichiometric hafnium dioxide (HfO_2) and (2) cubic of space group I a − 3 with the chemical composition of Hf_2N_2O, as shown in Fig. 8. However, care must be taken during structure determination. Due to the small thickness of the investigated material, the collected patterns have very broad peak shape. For that reason, reflexes originating from various phases can overlap with each other. Moreover, some of the peaks, with a certain degree of probability, can be attributed to various other phases such as HfO_2 orthorhombic (space group P b c m), HfO_2 cubic (group space F m − 3 m) or $Hf_{2.01}N_{2.68}$ tetragonal (space group I 4/m). Indeed, the simultaneous presence of two or more various phases in hafnium oxide and oxynitride thin-films is widely reported [36–39]. Nevertheless, for the phases identified in this work, the ratio between the monoclinic and cubic phase can be estimated at the level ~ 79/21%.

Moreover, the AFM studies proved that the increase in crystalline phases in the layer bulk has not deteriorated the surface morphology and the homogeneity of the thickness of investigated dielectric films, as it was depicted in Fig. 8. It is worth noting that the change of RMS values due to the annealing is negligible, and the surface of consecutive HfO_xN_y films shows similar topography.

The structural rebuilt and the increase of the crystalline phase present in the hafnium oxynitride bulk that is reported in this study can be attributed to the improvement of the electrical properties of MIS structures. The deterioration of the electrical behavior of high-*k* materials due to the significant increase of the crystalline phase as a consequence of high-temperature treatment, which was demonstrated in the literature [40,41], was not observed in our work. The literature reports thermally stable gate-dielectric high-*k* films, e.g. ALD HfO_xN_y [42] or HfSiON [43] with high-quality electrical properties, which is related to the stability of the amorphous phase of dielectric material bulk. However, the results presented in this study have proved that although the phase of sputtered hafnium oxynitride after the high-temperature treatment can be characterized by crystalline nature with the inclusion of amorphous phase, the electrical properties can be still improved as compared to reference test structures.

This is due to the rebuild of the structure of hafnium oxynitride films that was observed after structural analysis, improved

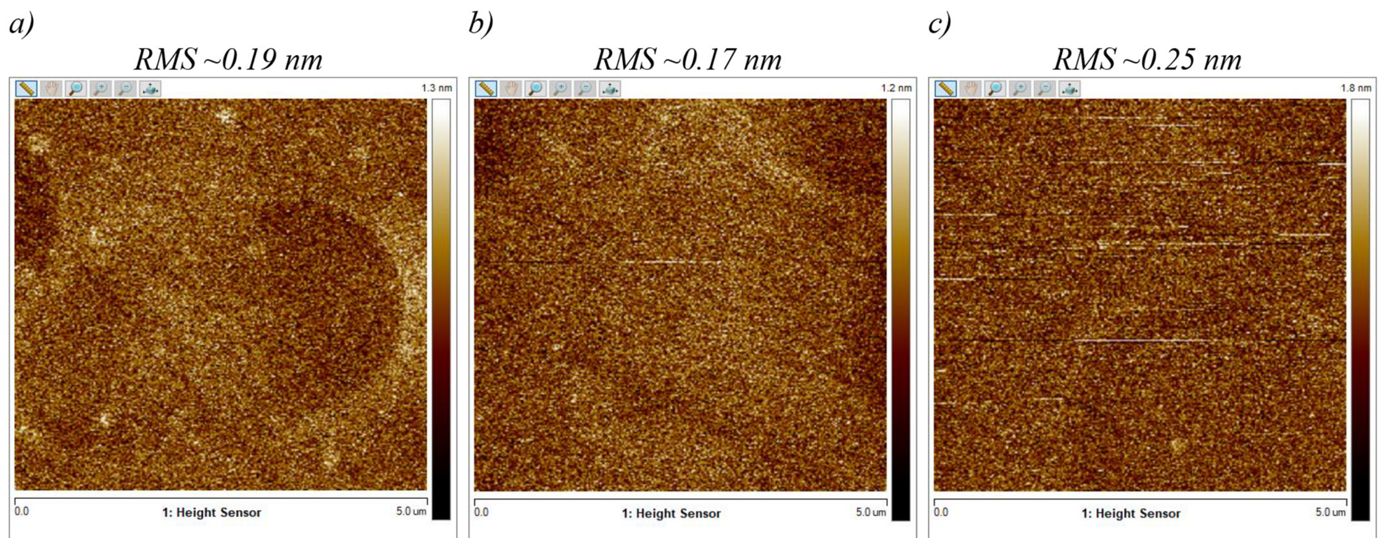

Fig. 8. Morphology of studied in this work HfO_xN_y films characterized by AFM: as-deposited (a), annealed at 300 °C (b), and 800 °C (c); corresponding RMS values were also shown.

crystallization temperature and the suppression of interfacial layer growth due to the presence of Si—N bonds in the dielectric/semiconductor interface [44,45]. The changes in surface morphology of HfO_xN_y layers were not also observed, as it was shown after AFM examinations. The results presented in this work have clearly proved the thermal stability of pulsed-DC reactively sputtered hafnium oxynitride films and make the fabricated film as a candidate in the application in the technology of MIS devices, e.g. in self-aligned technology as the gate-dielectric material.

4. Conclusion

The Design of Experiments method using Taguchi orthogonal tables has been used to choose a set of process' parameters of hafnium oxynitride films with the best possible electrical properties. The optimized dielectric films have been formed by pulsed-DC reactive magnetron sputtering. The performed experimental runs allowed for the analysis of the influence of process' parameters onto electrical and structural properties of investigated thin-films. The thermal stability of HfO_xN_y was also examined and the superior stability of deposited films up to 800 °C was demonstrated. The analysis of obtained C—V and J-E characteristics of MIS structures confirmed the improvement of electrical parameters of dielectric films, i.e. the lower effective charge density, lower interface states density, as well as lower flat-band voltage (in absolute values). Moreover, the insulating properties and breakdown voltage value of hafnium oxynitride films were also improved, although the relative permittivity has slightly decreased compared to samples without any thermal treatment. Structural analysis of dielectric thin-films revealed the increase of the crystalline phase in the bulk of dielectric material, however, no deterioration of electrical properties of MIS structures was observed. The findings presented in this work make the investigated dielectric material the possible candidate as a gate dielectric in MOS/MIS structures and devices.

Declaration of Competing Interest

None.

Acknowledgments

This work has been partially supported by The National Centre for Research and Development (NCBiR) under grant No. TECHMATSTRATEG1/347012/3/NCBR/2017 (HYPERMAT) in the course of “Novel technologies of advanced materials – TECHMATSTRATEG”.

References

[1] G.D. Wilk, R.M. Wallace, M. Anthony, J. Appl. Phys. 89 (2001) 5243–5275.
[2] J. Robertson, R.M. Wallace, Mater. Sci. Eng. R. Rep. 88 (2015) 1–41.
[3] N.-W. Pi, M. Zhang, J. Jiang, A. Belosludtsev, J. Vlček, J. Houška, E.I. Meletis, Thin Solid Films 619 (2016) 239–249.
[4] J. Robertson, Solid-Stat. Electron. 49 (3) (2005) 283–293.
[5] G. Groeseneken, L. Pantisano, L.-Å. Ragnarsson, R. Degraeve, M. Houssa, T. Kauerauf, P. Roussel, S. De Gendt, M. Heyns, Proc. 11th IPFA, Hsinchu, Taiwan, R.O.C, 2004, pp. 147–155.
[6] S.J. Lee, H.F. Luan, W.P. Bai, C.H. Lee, T.S. Jeon, Y. Senzaki, D. Roberts, D.L. Kwong, IEDM Tech. Dig. (2000) 31–34.
[7] J.K. Shaeffer, S.B. Samavedam, D.C. Gilmer, V. Dhandapani, P.J. Tobin, J. Mogab, B.-Y. Nguyen, B.E. White Jr., S. Dakshina-Murthy, R.S. Rai, Z.-X. Jiang, R. Martin, M.V. Raymond, M. Zavala, L.B. La, J.A. Smith, R. Garcia, D. Roan, M. Kottke, R.B. Gregory, J. Vac, Sci. Technol. (B) 21 (1) (2003) 11–17.
[8] B.H. Lee, L. Kang, R. Nieh, W.J. Qi, J.C. Lee, Appl. Phys. Lett. 76 (2000) 1926.
[9] M. Cao, P.V. Voorde, M. Cox, M. Greene, IEEE Electron. Dev. Lett. 19 (1998) 291.
[10] C.S. Kang, H.-J. Cho, K. Onishi, R. Choi, Y.H. Kim, R. Nieh, J. Han, S. Krishnan, A. Shahriar, J.C. Lee, IEDM Tech. Dig 865 (2002) 2002.
[11] M. Lee, Z.-H. Lu, W.-T. Ng, D. Landeer, X. Wu, S. Moisa, Appl. Phys. Lett. 83 (2003) 2638.
[12] C.S. Kang, H.J. Cho, K. Onishi, R. Nieh, R. Choi, S. Gopalan, Appl. Phys. Lett. 81 (2002) 2593.
[13] K.J. Chio, J.H. Kim, S.G. Yoon, W.C. Shin, J. Vac. Sci. Technol. B 22 (2004) 1755.
[14] J.F. Kang, H.Y. Yu, C. Ren, M.F. Li, D.S.H. Chan, H. Hu, Appl. Phys. Lett. 84 (2004) 1588.
[15] A. Obstarczyk, D. Kaczmarek, D. Wojcieszak, M. Mazur, J. Domaradzki, T. Kotwica, R. Pastuszek, D. Schmeisser, P. Mazur, M. Kot, Mater. Des. 175 (2019) 107822.
[16] A. Belosludtsev, J. Houška, J. Vlček, S. Haviar, R. Čerstvy, J. Rezek, M. Kettner, Ceram. Int. 43 (7) (2017) 5661–5667, https://doi.org/10.1016/j.ceramint.2017.01.102.
[17] G.Z. Yin, Orthogonal Design for Process Optimization and its Application in Plasma Etchnig, Intel Corp, 1986.
[18] L.M. Lye, Tools and toys for teaching design of experiments methodology, 33rd Annual General Conference of the Canadian Society for Civil Engineering, 2005 Toronto, Ontario, Canada.
[19] D.C. Montgomery, Design and Analysis of Experiments, Wiley, New York, 2005.
[20] L. Ilzarbe, Qual. Reliab. Eng. Int. 24 (4) (2008) 417–428.
[21] A. Dean, D. Voss, D. Draguljić, Design and Analysis of Experiments, 2nd edition, Springer, 2017, https://doi.org/10.1007/978-3-319-52250-0.
[22] R. Storn, K. Price, J. Glob. Optim. 11 (4) (1997) 341–359 Dec.
[23] N. Daneshvar, A.R. Khataee, M.H. Rasoulifard, M. Pourhassan, J. Hazard. Mater. 143 (1–2) (2007) 214–21922.
[24] S.M. Tasirin, S.K. Kamarudin, J.A. Ghani, K.F. Lee, J. Food Eng. 80 (2) (2007) 695–700.
[25] C.-H. Wu, W.-S. Chen, Sens. Actuat. A: Phys. 125 (2) (2006) 367–375.
[26] J.-Y. Houng, J.-H. Liao, J.-Y. Wu, S.-C. Shen, H.-F. Hsu, Process Biochem. 42 (1) (2007) 1–7.
[27] R. Romero-Villafranca, L. Zúnica, R. Romero-Zúnica, J. Statist. Plan. and Inferen

137 (4) (2007) 1488–1495.
[28] A.K. Elshennawy, Total Qual, Manag. Bus. Excell. 15 (5–6) (2004) 603–614.
[29] E.Y.K. Ng, W.K. Ng, Med. Biolog. Engin. Comp. 44 (1–2) (2006) 131–139.
[30] R. Mroczyński, R.B. Beck, ECS Trans. 25 (8) (2009) 797–804.
[31] R. Mroczyński, M. Kalisz, M. Dominik, Phys. Status Solidi C (2016) 1–6.
[32] M. Szymańska, S. Gierałtowska, Ł. Wachnicki, M. Grobelny, K. Makowska, R. Mroczyński, Appl. Surf. Sci. 301 (2014) 28–33.
[33] A. Belosludtsev, Y. Yakimov, R. Mroczyński, S. Stanionytė, M. Skapas, D. Buinovskis, N. Kyžas, Phys. Status Solidi A (2019) 1900122.
[34] T. Ino, Y. Kamimuta, M. Suzuki, M. Koyama, A. Nishiyama, Jap. J. App. Phys. 45 (4B) (2006) 2908–2913.
[35] E. Atanassova, M. Georgieva, D. Spassov, A. Paskaleva, Microelectron. Eng. 87 (2010) 668–676, https://doi.org/10.1016/j.mee.2009.09.006.
[36] W. Liu, X. Su, S. Zhang, H. Wang, J. Liu, L. Yan, Vacuum. 82 (2008) 1280–1284.
[37] P. Polakowski, M. Johannes, Appl. Phys. Lett. 106 (2015).
[38] K. Sarakinos, D. Music, S. Mraz, M. Baben, K. Jiang, F. Nahif, A. Braun, C. Zilkens, S. Konstantinidis, F. Renaux, D. Cossement, F. Munnik, J.M. Schneider, J. Appl. Phys. 108 (2015).
[39] C. Wiemer, S. Ferrari, M. Fanciulli, G. Pavia, L. Lutterotti, Thin Solid Films 450 (2004) 134–137.
[40] L. Pereira, P. Barquinha, E. Fortunato, R. Martins, Mater. Sci. Semicond. Process. 9 (2006) 1125–1132.
[41] A. Taube, R. Mroczyński, K. Korwin-Mikke, S. Gierałtowska, J. Szmidt, A. Piotrowska, Mater. Sci. Eng. B 177 (2012) 1281–1285.
[42] M.A. Quevedo-Lopeza, S.A. Krishnan, P.D. Kirschb, G. Pant, B.E. Gnade, R.M. Wallace, Appl. Phys. Lett. 87 (2005) 262902.
[43] X. Wang, J. Liu, F. Zhu, N. Yamada, Dim-Lee Kwong, IEEE Trans. Elec. Dev. 51 (11) (2004) 1798–1804.
[44] G. Hea, Q. Fang, L.D. Zhang, Mater. Sci. Semicond. Process. 9 (2006) 870–875.
[45] D. Gui, J. Kang, H. Yu, H.F. Lim, App. Surf. Scien. 231–232 (2004) 590–595.